Engineering and Applied Sciences
2026, Vol. 11, No. 4, pp. 105–114
https://doi.org/10.11648/j.eas.20261104.11

Research Article

# Process Planning and Precision Fabrication of an Aluminum Linkage Arm by CNC Milling and Wire EDM

**Tran Thanh Tung[1], Nguyen Thi Anh[2], Nguyen Xuan Quynh[3], Tran Vu Minh[3, *]**

[1]Faculty of Engineering Mechanics and Automation, VNU University of Engineering and Technology, Hanoi, Vietnam
[2]Faculty of Mechanical Engineering, Thuyloi University, Hanoi, Vietnam
[3]School of Mechanical Engineering, Hanoi University of Science and Technology, Hanoi, Vietnam

## Abstract

Linkage arms containing a keyed bore, forked end, pivot hole, and tapered web require coordinated datum control and machining sequence because setup transfer and local stiffness variation can degrade geometric accuracy. This study develops and experimentally evaluates a requirement-driven process-planning framework for the low-volume manufacture of a precision linkage arm from 6061-T6 aluminum alloy using three-axis computer numerical control (CNC) milling and wire electrical discharge machining (WEDM). The objective is to translate the functional requirements into an auditable chain covering datum selection, allowance distribution, tool choice, setup sequence, machining conditions, and final inspection. A single component was fabricated on a VF-1 vertical machining center. The route comprised primary and secondary face generation, staged roughing and finishing, contour milling, circular interpolation, reaming, reverse-side re-fixturing through previously machined features, chamfering, and final WEDM of the internal keyway. The principal bore was completed before WEDM to reference the keyway to the actual bore axis and retain stiffness during bulk material removal. Inspection showed that the principal bore and pivot-hole diameters and the local section thicknesses conformed to the drawing requirements. The reported parallelism deviation was 0.04 mm, while the hole-axis-to-end-face non-perpendicularity was 0.06 mm. A preliminary screening error budget indicated that primary-datum generation and reverse-side re-fixturing accounted for approximately 55–60% of these deviations, identifying setup transfer as the dominant improvement target. The results demonstrate that accuracy depended on datum continuity, controlled re-fixturing, and correct multi-process sequencing rather than on any single operation. The proposed framework provides a practical and traceable basis for low-volume linkage-component manufacture, although repeated trials, formal uncertainty analysis, surface metrology, and mechanical validation remain necessary before industrial process capability can be established.

## Keywords

Linkage Arm, CNC Milling, Wire Electrical Discharge Machining, Process Planning, Dimensional Accuracy, Aluminum Alloy

*Correspondence: Tran Vu Minh (minh.tranvu@hust.edu.vn)

**Received:** 13 July 2026; **Accepted:** 23 July 2026; **Published:** 10 August 2026

## 1. Introduction

Computer numerical control (CNC) milling is widely used to manufacture mechanical components containing planar datums, free contours, bores, slots, and locally slender features. However, final accuracy is not determined by machine capability alone; it emerges from the coordinated selection of datum structure, machining allowance, toolpath, cutting conditions, workholding, and inspection. Existing studies have optimized cooling, cutting parameters, and data-driven process settings [1-3], while prototype-machine development and compensation research have shown that machine architecture and geometric, thermal, and tool-deflection errors also affect the manufactured geometry [4, 5]. These contributions provide important operation-level solutions, but they generally evaluate individual variables rather than the complete dependency chain among the functional features of a specific part.

Research on digital manufacturing has advanced sustainability assessment, robotic milling, contour programming, and machine-tool implementation [6-10], together with feed-rate control, precision compensation, post-processing, computer-aided design and computer-aided manufacturing (CAD/CAM) integration, and accessible machining simulation [11-15]. STEP-NC and model-continuity studies further demonstrate that data integrity is essential for reliable machining [16, 17]. Nevertheless, these methods do not by themselves specify how a workshop should establish datums, retain stiffness, distribute stock, transfer setups, and schedule a non-milling process for a single linkage component with coupled bore, keyway, fork, and face requirements.

The challenge becomes more pronounced when the workpiece has a variable cross-section and an open fork. Models for flatness error, dynamic deformation, finite-element parameter assessment, validated thin-wall simulation, micro-milling deflection, and position-dependent dynamics have quantified the sensitivity of low-stiffness structures to machining loads [18-23]. Experimental and numerical studies have additionally shown that surface topography, cutting strategy, cutter-workpiece engagement, milling direction, force-deflection coupling, and process optimization influence the final error [24-31]. Collectively, this literature establishes that support conditions and material-removal sequence are decisive; however, most studies address benchmark thin walls or optimize a particular response rather than a linkage arm that combines stiff bosses, a tapered web, and an interrupted fork within one datum network.

Residual-stress studies and fixture-force analysis have further clarified the roles of initial stress, distortion compensation, and clamping in dimensional variation [32-35]. Related work on allowance planning, CNC automation, and Taguchi-based parameter optimization provides useful tools for individual planning decisions [36-38], whereas wire electrical discharge machining (WEDM) offers a force-free route for narrow internal features [39]. A clear methodological gap nevertheless remains: the cited literature does not provide a fully traceable manufacturing chain that converts the drawing of a linkage arm into datum selection, allowance distribution, setup transfer, CNC operations, WEDM sequencing, and feature-based inspection. The present contribution addresses this gap through an application-oriented and auditable process-planning case study rather than by proposing another cutting-force or optimization model.

Accordingly, the objectives are to (i) identify the functional features and associated geometric requirements; (ii) develop a compact CNC-WEDM route suitable for single-unit production; (iii) explain the selection of setups, tools, allowances, and machining conditions; (iv) assess whether the completed component satisfies the reported dimensional and geometric requirements; and (v) provide a preliminary error-budget interpretation of the measured deviations. The principal novelty is the explicit linkage of design requirements, datum continuity, feature dependency, multi-process sequencing, and inspection within one verifiable manufacturing framework.

## 2. Materials and Methods

### 2.1. Component Design and Manufacturing Requirements

The investigated part is a linkage arm used to transmit force and rotational or oscillatory motion between two mechanical joints. Figure 1 shows the overall CAD geometry. The left-hand fork contains the principal circular interface and an internal keyway, while the opposite end contains the secondary pivot hole. The tapered web reduces mass between the two functional ends, but it also creates a non-uniform stiffness distribution. The open slot divides the large end into two arms; hence excessive clamping or an unsuitable machining order can change the fork opening and degrade the parallelism of the two branches.

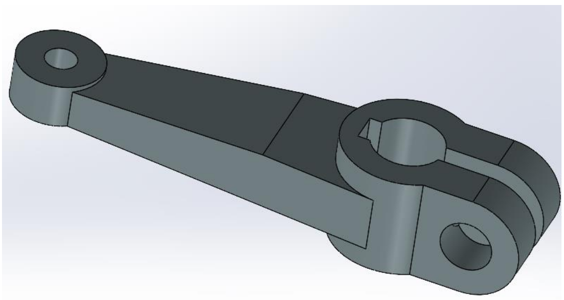

***Figure 1.*** *Three-dimensional CAD model of the mechanical linkage arm.*

The drawing in Figure 2 was interpreted as a functional chain rather than only as a list of dimensions. The central bore and keyway establish shaft location and torque transfer. The secondary hole establishes the pivot axis and, together with the main bore, controls the effective center distance of the linkage. The end faces provide assembly contact and define the axial position of mating components. The 15, 20, and 16 mm local thicknesses govern the relative position of these faces, while the fork slot must remain symmetric about the central bore. For this reason, the broad faces and the principal bore were treated as manufacturing datums from which the remaining geometry was generated.

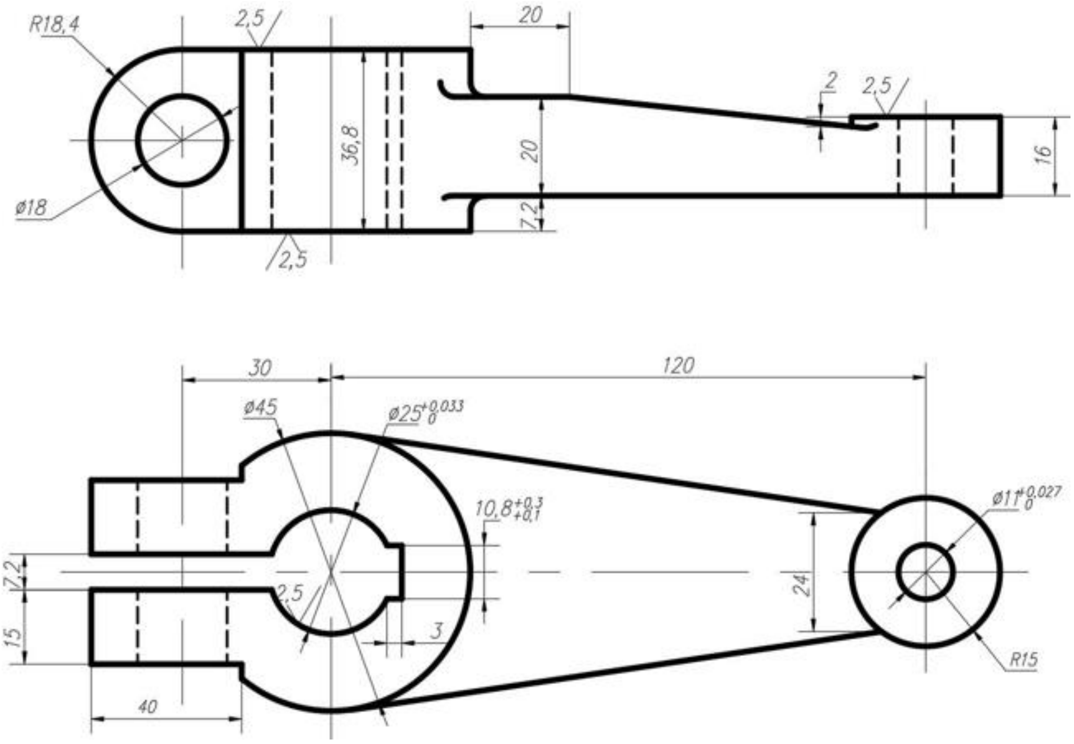


*Figure 2. Technical drawing and principal dimensions of the linkage arm.*

*Table 1. Functional features and manufacturing implications.*

| Feature | Functional requirement | Primary risk | Process-planning response |
|---|---|---|---|
| Central keyed bore | Shaft location and torque transfer | Bore/keyway misalignment | Finish bore before WEDM; reference keyway to bore axis |
| Fork opening | Clearance and two-arm load transfer | Branch deflection and loss of parallelism | Retain stock during early cuts; finish from stable datums |
| Pivot hole | Secondary rotational joint | Center-distance and axis-position error | Machine in same coordinate chain as principal bore |
| Tapered body | Mass reduction with adequate stiffness | Changing stiffness during material removal | Rough before opening fork; use low finishing allowance |
| Reference faces / local thicknesses | Axial assembly location | Face-to-hole perpendicularity error | Generate primary and secondary faces before precision features |

The prototype was manufactured from an available aluminum blank and reported as 6061-T6 in the component specification. Aluminum was appropriate for the single-unit study because of its low density, corrosion resistance, and good machinability. The source process plan initially considered near-net-shape routes for higher production volumes, but a prismatic blank was selected to reduce tooling cost and lead time. The blank allowance was distributed as approximately

2.5 mm on the upper face, 2.0 mm on the lower face, and 2.2 mm on the side surfaces. This distribution provided sufficient stock for establishing reference planes and removing blank irregularities before finishing.

The technological route was derived from feature dependency. First, a broad face was generated to provide a stable primary datum. The opposite face was then machined to establish thickness and parallel reference surfaces. The external profile and main circular features were produced while the blank retained maximum stiffness. The primary bore was finished before the internal keyway so that the keyway could be referenced to the actual bore axis. The part was subsequently reversed and located through already machined features to finish the remaining faces and fork geometry. Chamfers were added after the critical diameters had been stabilized, and WEDM was reserved for the narrow internal keyway. Final inspection followed the same datum chain used during machining.

## 2.2. Integrated Machining Procedure

The complete CNC sequence is summarized in Figure 3. In the first setup, the blank was clamped in a mechanical vise on the VF-1 machining center. Rough face milling removed approximately 2 mm using a 10 mm end mill at about 4000 rpm and 3000 mm/min. Semi-finishing was performed with an 8 mm end mill at about 5000 rpm and 600 mm/min, followed by a finishing pass using a 6.5 mm corner-radius tool at approximately 5539 rpm and 2309 mm/min with a 0.2 mm finishing allowance. The principal bore was then finished by reaming at approximately 3000 rpm and 100 mm/min. This staged sequence established the face datum and bore axis before a substantial reduction in section stiffness occurred.

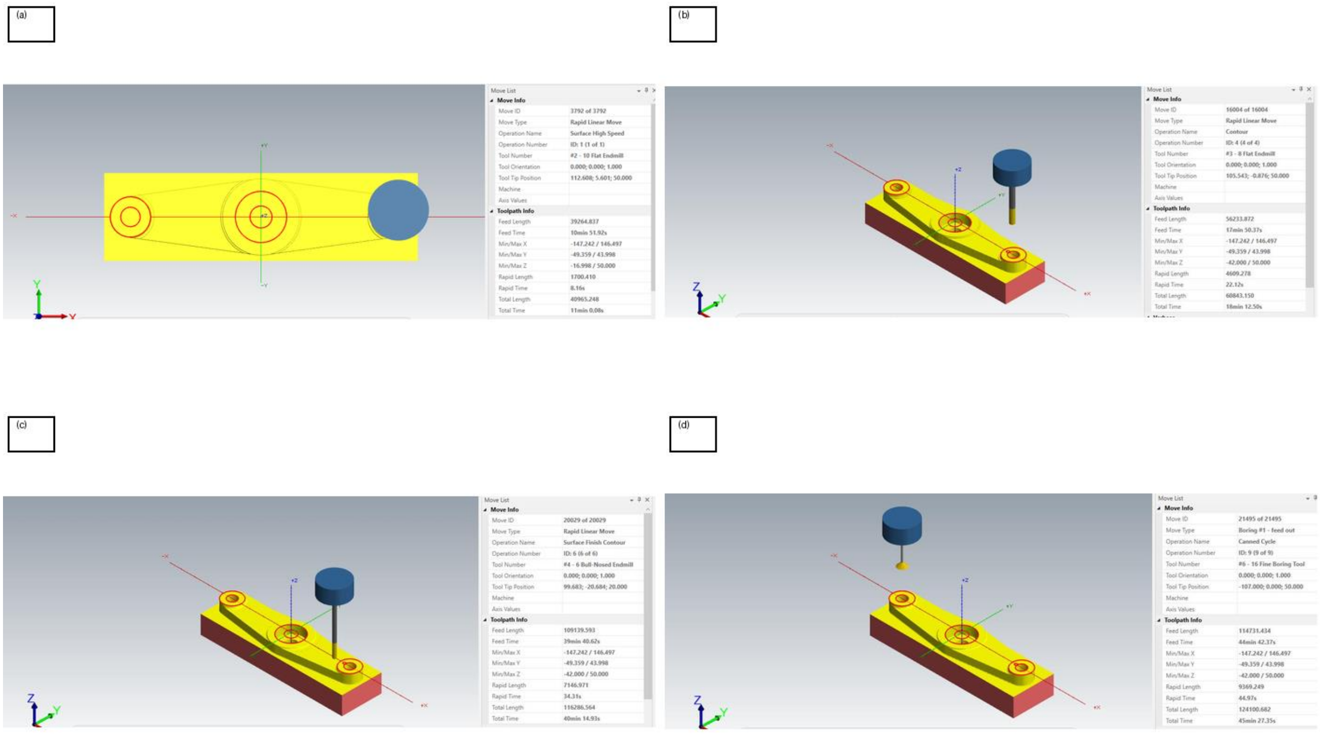


***Figure 3.*** *CAM-based machining sequence: (a) initial face roughing, (b) semi-finishing and finishing of the reference face, (c) reaming and contour generation, and (d) reverse-side machining and completion of the remaining surfaces.*

Figure 4 presents two stages that belong to the actual machining route of the clamp-type linkage arm. The first-side operation was programmed in CAM to rough the external profile and establish the principal reference geometry. After the main holes and contour had been generated, the workpiece was inverted and located through the previously machined feature, then secured by a threaded fastener for reverse-side roughing and finishing. This re-fixturing strategy preserved the relationship between the two faces while providing unobstructed tool access to the remaining stock.

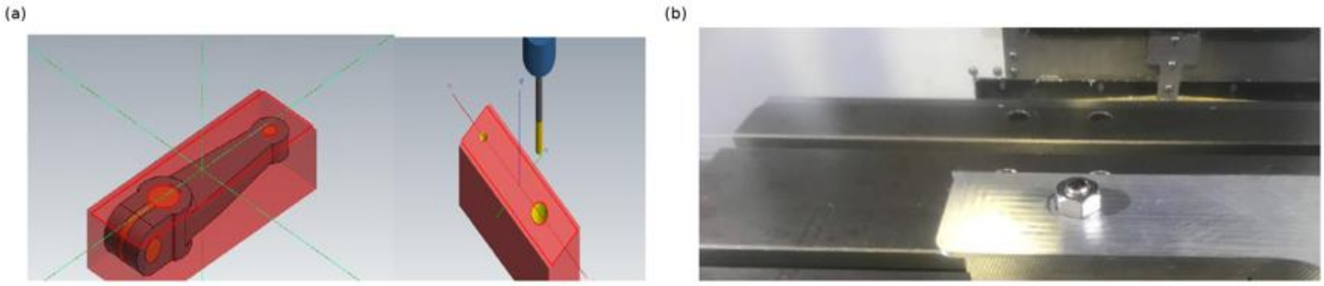


*Figure 4. Machining stages of the clamp-type linkage arm: (a) CAM simulation of the hole-machining operation on the first side and (b) reverse-side setup using a threaded fastener after the primary contour and locating features had been machined.*

*Table 2. Principal machining conditions used in the fabrication route.*

| Operation | Tool/process | Tool size | Spindle speed | Feed rate | Allowance/depth |
|---|---|---|---|---|---|
| First-side roughing | Flat end milling | D10 mm | 4000 rpm | 3000 mm/min | ~2.0 mm rough stock |
| Semi-finishing / finishing | End milling | D8 / D6.5 | 5000 / 5539 rpm | 600 / 2309 mm/min | ~2.0 mm semi-finish; 0.2 mm finish |
| Principal-bore finishing | Reaming | D16 in source route | 3000 rpm | ~100 mm/min | Final bore sizing |
| Reverse-side rough/finish | End milling | D10.4 / D6.5 | 4200 / 5539 rpm | 4000 / 2309 mm/min | 0.5 mm rough; 0.2 mm finish |
| Chamfering | Chamfer milling | D6 mm | 6000 rpm | ~1000 mm/min | 3 x 45° feature |
| Internal keyway | Wire EDM | 0.18 mm Mo wire | — | — | 200 mm/min cutting speed |

The internal slot and keyed bore features were produced after completion of the principal milled surfaces and holes. As shown in Figure 5, the actual clamp-type linkage arm was mounted on the wire electrical discharge machining (WEDM) table, with the cutting path referenced to the previously machined bore and external datums. A 0.18 mm molybdenum wire and a nominal cutting speed of 200 mm/min were used. WEDM was selected because the narrow internal geometry and the forked end are difficult to finish with a conventional rotating tool without additional access or dedicated broaching equipment. Performing this operation after CNC milling also prevented premature reduction of stiffness around the fork during the main material-removal stages.

*Figure 5. WEDM machining of the internal slot and keyed-bore features of the clamp-type linkage arm.*

Inspection was organized according to the functional datum chain defined by the drawing. The principal checks included the diameters of the Ø25 mm keyed bore and Ø11.8 mm pivot hole, the local section thicknesses of 15, 20, and 16 mm, the relative alignment of the functional holes, and conformity of the WEDM-generated slot geometry. The source record reports that the hole diameters and section thicknesses remained within their specified dimensional limits and that the parallelism deviation of the basic holes was 0.04 mm. Surface roughness, however, was not fully verified against the original cast-iron-oriented specification because the prototype was manufactured from an available aluminum blank. The dimensional results should therefore be interpreted as validation of the selected datum and machining sequence rather than as a complete qualification of surface integrity. *The source record additionally reported a hole-axis-to-end-face non-perpendicularity of 0.06 mm.*

## 3. Results

Figure 6 shows the completed clamp-type linkage arm corresponding to the CAD model and technical drawing in Figures 1 and 2. The manufactured component preserves the tapered body, forked end, keyed central bore, and opposite pivot hole of the investigated design. Visual comparison with the drawing confirms that the process sequence generated the intended external contour and maintained the separation and symmetry of the fork arms. Dimensional inspection reported conformity of the functional hole diameters and the 15, 20, and 16 mm local thicknesses, together with a 0.04 mm parallelism deviation between the basic holes. The completed part therefore demonstrates the direct relationship between the functional requirements, the datum-based CNC sequence, and the final WEDM operation. The measured hole-axis-to-end-face non-perpendicularity was 0.06 mm.


***Figure 6.*** *Completed aluminum clamp-type linkage arm after CNC milling and WEDM. The 50 mm reference scale was calibrated from the 120 mm center distance specified in Figure 2.*

## 4. Discussion

***Table 3.*** *Summary of dimensional and geometric inspection.*

| Characteristic | Nominal/drawing requirement | Inspection result | Assessment |
|---|---|---|---|
| Central bore diameter | Ø25 mm within drawing tolerance | Within specified tolerance | Conforming |
| Pivot hole diameter | Ø11.8 mm within drawing tolerance | Within specified tolerance | Conforming |
| Local section thicknesses | 15, 20, and 16 mm | Matched nominal drawing values | Conforming |
| Parallelism of basic holes | Per drawing requirement | 0.04 mm | Acceptable |
| *Hole-axis-to-end-face perpendicularity* | *Per drawing requirement* | *0.06 mm* | *Acceptable* |
| Surface roughness | Drawing-specific Ra/Rz requirement | Not fully verified for the aluminum prototype | Requires further measurement |
| Internal slot/keyed-bore geometry | Drawing geometry and position | Conformed visually and | Conforming |

| Characteristic | Nominal/drawing requirement | Inspection result | Assessment |
|---|---|---|---|
| | | dimensionally to the source drawing | |

The results demonstrate a direct correspondence between the design requirements in Figures 1 and 2 and the operations in Figures 3-5. The requirement for controlled face-to-hole relationships led to face generation before precision-hole finishing. The need to preserve center distance led to machining both circular interfaces from a stable coordinate system. The fork-parallelism requirement led to retaining material during early operations and postponing the open-slot completion until reliable datums were available. Finally, the requirement for an accurately positioned internal keyway led to finishing the main bore before WEDM.

The process route also clarifies why the final quality cannot be attributed to WEDM or CNC milling alone. CNC milling established the datum planes, external contour, bore positions, and local thicknesses. Reaming stabilized the principal bore geometry, while WEDM generated the internal keyway without imposing significant cutting force on the fork. The 0.04 mm parallelism and 0.06 mm perpendicularity outcomes therefore represent the cumulative effect of datum preservation, setup transfer, clamping, allowance control, and final feature sequencing.

To provide a first-order quantitative interpretation of the reported geometric deviations, a screening error budget was constructed from the sequence of datum creation, setup transfer, feature finishing, and inspection. Because only one component was produced and no repeated coordinate-metrology dataset was available, the values in Table 4 are proportional engineering allocations of the measured totals rather than independently measured uncertainty components. The allocation assumes linear accumulation and is intended to identify the dominant process stages, not to establish formal metrological traceability.

***Table 4.*** *Preliminary screening allocation of the reported geometric deviations.*

| Error source | Dominant mechanism | Parallelism allocation | Perpendicularity allocation |
|---|---|---|---|
| Primary datum generation | Reference-face flatness and orientation | 0.008 mm (20%) | 0.015 mm (25%) |
| Reverse-side re-fixturing | Datum transfer and locating repeatability | 0.014 mm (35%) | 0.021 mm (35%) |
| Clamping and local compliance | Elastic response of the tapered body and fork | 0.008 mm (20%) | 0.009 mm (15%) |
| Hole finishing and tool-axis alignment | Reaming alignment, runout, and interpolation error | 0.006 mm (15%) | 0.009 mm (15%) |
| Inspection contribution | Instrument resolution and operator alignment | 0.004 mm (10%) | 0.006 mm (10%) |
| Linear screening total | Allocated to the reported final deviations | 0.040 mm (100%) | 0.060 mm (100%) |

The screening allocation indicates that primary-datum generation and reverse-side re-fixturing account for an estimated 55% of the 0.04 mm parallelism deviation and 60% of the 0.06 mm perpendicularity deviation. The second setup is therefore the highest-priority target for improvement. More repeatable location through precision pins, controlled tightening torque, and coordinate-measuring-machine verification after each setup would allow these allocations to be tested experimentally in a subsequent batch.

Allowance distribution was equally important. The initial upper, lower, and side allowances provided enough stock to establish clean datums, while the 0.2 mm finishing allowance limited the cutting load during the final passes. This is consistent with recent work showing that machining allowance should be treated as a process variable because excessive finishing stock increases force, time, and deformation, whereas insufficient stock cannot remove roughing-induced errors [36]. The adopted values were not mathematically optimized, but they formed a practical compromise compatible with the available machine, tools, and single-unit production environment.

The evidence remains dimensional and technological rather than structural. The present study verifies that the selected route can produce one conforming component; it does not establish fatigue strength, torque capacity, wear resistance, or statistical process capability. Moreover, the original manufacturing record contains two related drawing variants with different nominal bore sizes. The revised article therefore reports the final component geometry from Figures 1 and 2 while using the earlier process record only for operations, parameter ranges, allowances, setup logic, and verified geometric deviations.

Compared with studies based on Taguchi optimization or multi-objective algorithms [36, 38], the present route uses workshop-feasible parameters selected from tool data, calculations, and machining trials. This limits generalization but strengthens the practical traceability of the case study. The spindle speeds of approximately 3000-6000 rpm and feed rates of 100-4000 mm/min span distinct process functions: low-feed reaming for bore quality, moderate-feed finishing for dimensional control, and high-feed roughing for productivity. Such separation is preferable to applying one parameter set indiscriminately to all features.

The workholding logic is consistent with established fixture-force principles [35]. Broad contact in the vise was used while the blank retained high stiffness, whereas machined holes and faces were used during the second setup to improve repeatability. This progression reduced reliance on irregular raw surfaces and avoided excessive force on the open fork. The same mechanism is repeatedly observed in variable-stiffness machining, where distributed support and controlled clamping are required to limit elastic deformation [18-31].

Several limitations remain. Only one component was manufactured, so repeatability and process capability indices cannot be calculated. Surface roughness was specified or qualitatively assessed but was not documented through a complete measurement dataset. The inspection record does not provide uncertainty, gauge repeatability and reproducibility, or coordinate-measuring-machine data. Mechanical validation under torsion, bending, cyclic loading, and assembled motion was also outside the scope. These limitations should be stated explicitly because dimensional conformity alone does not prove long-term structural reliability.

Future work should manufacture a statistically meaningful batch, apply coordinate-measuring-machine inspection to the complete feature network, and report surface roughness at the bore, end faces, fork slot, and keyway. Cutting-force acquisition and tool-wear monitoring would help explain the selected parameters, while finite-element analysis and mechanical testing could verify the stress concentration at the fork-to-web transition. A comparison of alternative datum schemes and clamping forces would further quantify the contribution of setup transfer to the final 0.04-0.06 mm geometric deviations.

## 5. Conclusions

A requirement-driven CNC-WEDM process was developed for a precision aluminum linkage arm. The technical drawing was converted into a manufacturing chain in which reference faces were generated first, the principal bore and secondary pivot were machined from stable datums, the component was reversed using already finished features, and the internal keyway was completed by WEDM only after the bore geometry had been stabilized. The source process data provided upper, lower, and side allowances of approximately 2.5, 2.0, and 2.2 mm, respectively, with a final allowance near 0.2 mm and operation-specific spindle speeds and feeds. The manufactured component conformed to the reported critical dimensions, with a fork-feature parallelism deviation of 0.04 mm and a hole-axis-to-face non-perpendicularity of 0.06 mm. A preliminary screening allocation attributed approximately 55-60% of these deviations to primary-datum generation and reverse-side re-fixturing, identifying setup transfer as the principal opportunity for process improvement. These results support the central conclusion that dimensional quality resulted from control of feature dependency and datum continuity rather than from any single machining operation. The approach is suitable as a practical basis for low-volume production, although repeated trials, formal uncertainty analysis, and mechanical validation are required before industrial capability can be claimed.

## Abbreviations

| | |
|---|---|
| CNC | Computer Numerical Control |
| WEDM | Wire Electrical Discharge Machining |
| CAD | Computer-Aided Design |
| CAM | Computer-Aided Manufacturing |

## Author Contributions

**Tran Thanh Tung:** Conceptualization, Investigation, Methodology, Project administration, Writing – original draft

**Nguyen Thi Anh:** Data curation, Formal Analysis, Methodology, Writing – review & editing

**Nguyen Xuan Quynh:** Investigation, Resources, Validation

**Tran Vu Minh:** Supervision, Validation, Writing – review & editing

## Data Availability Statement

The data supporting the outcome of this research work has been reported in this manuscript. Additional manufacturing records are available from the corresponding author upon reasonable request.

## Conflicts of Interest

The authors declare no conflicts of interest.

## References

[1] A. S. Patil, V. K. Sunnapwar, K. S. Bhole, M. P. Ray, and Y. S. More, “Effective cooling methods for Ti-6Al-4V CNC milling: A review,” Advances in Materials and Processing Technologies, vol. 9, no. 2, pp. 457-506, 2023, https://doi.org/10.1080/2374068X.2022.2094073

[2] P. G. Mongan et al., "An ensemble neural network for optimising a CNC milling process," Journal of Manufacturing Systems, vol. 71, pp. 377-389, 2023, https://doi.org/10.1016/j.jmsy.2023.09.012

[3] A. Equbal et al., "Evaluating CNC milling performance for machining AISI 316 stainless steel with carbide cutting tool insert," Materials, vol. 15, no. 22, art. 8051, 2022, https://doi.org/10.3390/ma15228051

[4] T. T. Tung, N. T. Anh, and T. V. Minh, "Design and development of a prototype 3-axis CNC wood carving machine," International Journal of Advanced Technology and Engineering Exploration, vol. 12, no. 125, pp. 528-541, 2025, https://doi.org/10.19101/IJATEE.2024.111101739

[5] M. Soori and B. Arezoo, "Dimensional, geometrical, thermal and tool deflection errors compensation in 5-axis CNC milling operations," Australian Journal of Mechanical Engineering, vol. 22, no. 5, pp. 935-949, 2024, https://doi.org/10.1080/14484846.2023.2195149

[6] R. C. Reis et al., "Life cycle assessment of metal products: A comparison between wire arc additive manufacturing and CNC milling," Advances in Industrial and Manufacturing Engineering, vol. 6, art. 100117, 2023, https://doi.org/10.1016/j.aime.2023.100117

[7] W. Wang et al., "A state-of-the-art review on robotic milling of complex parts with high efficiency and precision," Robotics and Computer-Integrated Manufacturing, vol. 79, art. 102436, 2023, https://doi.org/10.1016/j.rcim.2022.102436

[8] Y. Petrakov, V. Korenkov, and A. Myhovych, "Technology for programming contour milling on a CNC machine," Eastern-European Journal of Enterprise Technologies, vol. 2, no. 1(116), pp. 55-61, 2022, https://doi.org/10.15587/1729-4061.2022.255389

[9] T. V. Minh, N. X. Quynh, N. T. Anh, and T. T. Tung, "Design and experimental study of a 4-axis CNC laser engraving machine," Journal of Engineering Sciences, vol. 54, no. 4, pp. 272-287, 2026, https://doi.org/10.21608/JESAUN.2025.423238.1737

[10] Z. Wang, X. Wang, X. Liu, et al., "Principle and application of the ball-end mill tool radius compensation for NURBS curve swept surfaces based on 3-axis CNC milling machines," International Journal of Precision Engineering and Manufacturing, vol. 22, pp. 1517-1526, 2021, https://doi.org/10.1007/s12541-021-00555-5

[11] J. Zhao and Z. Chang, "A new approach of modelling bottom-edge cutting in 4-axis rough milling of complex parts and its application on feed-rate optimization," Micromachines, vol. 13, art. 2071, 2022, https://doi.org/10.3390/mi13122071

[12] T. C. Chan, J. D. Li, U. Farooq, et al., "Improving machining accuracy of complex precision turning-milling machine tools," International Journal of Advanced Manufacturing Technology, vol. 131, pp. 211-227, 2024, https://doi.org/10.1007/s00170-024-13088-8

[13] S. H. Mohamed Said and M. S. Abu Mansor, "A study on post processor for 5-axis CNC milling via CAD/CAM system," in Intelligent Manufacturing and Mechatronics, Springer, 2022, pp. 451-461, https://doi.org/10.1007/978-981-16-8954-3_42

[14] X. Yan, "Research and application of CNC machining method based on CAD/CAM/robot integration," Advances in Multimedia, vol. 2022, art. 5397369, 2022, https://doi.org/10.1155/2022/5397369

[15] L. N. Misman and M. S. Abu Mansor, "Investigation on accessible CNC simulation approaches for multi-axis milling machining through CAD/CAM," in Intelligent Manufacturing and Mechatronics, Springer, 2024, https://doi.org/10.1007/978-981-97-0169-8_58

[16] M. Dharmawardhana, A. Ratnaweera, and G. Oancea, "STEP-NC compliant intelligent CNC milling machine with an open architecture controller," Applied Sciences, vol. 11, art. 6223, 2021, https://doi.org/10.3390/app11136223

[17] D. Kučera, I. Linkeová, and M. Stejskal, "The influence of CAD model continuity on accuracy and productivity of CNC machining," International Journal of Advanced Manufacturing Technology, vol. 124, pp. 1115-1128, 2023, https://doi.org/10.1007/s00170-022-10422-w

[18] A. Agarwal and K. A. Desai, "Modeling of flatness errors in end milling of thin-walled components," Proceedings of the Institution of Mechanical Engineers, Part B: Journal of Engineering Manufacture, vol. 235, no. 3, pp. 543-554, 2021, https://doi.org/10.1177/0954405420949214

[19] G. Ge et al., "An efficient prediction method for the dynamic deformation of thin-walled parts in flank milling," Computer-Aided Design, vol. 152, art. 103401, 2022, https://doi.org/10.1016/j.cad.2022.103401

[20] M. Hailong, T. Aijun, X. Shubo, and L. Tong, "Finite element simulation of bending thin-walled parts and optimization of cutting parameters," Metals, vol. 13, art. 115, 2023, https://doi.org/10.3390/met13010115

[21] N. T. Anh and T. T. Tung, "Development and validation of finite element model of milling thin-walled part," Applications in Engineering Science, vol. 25, art. 100285, 2026, https://doi.org/10.1016/j.apples.2025.100285

[22] Z. Jia et al., "Deflection prediction of micro-milling Inconel 718 thin-walled parts," Journal of Materials Processing Technology, vol. 291, art. 117003, 2021, https://doi.org/10.1016/j.jmatprotec.2020.117003

[23] B. Karimi and Y. Altintas, "Hybrid modeling of position-dependent dynamics of thin-walled parts using shell elements for milling simulation," Journal of Manufacturing Science and Engineering, vol. 144, no. 8, art. 081014, 2022, https://doi.org/10.1115/1.4053596

[24] S. Kurpiel, K. Zagórski, J. Cieślik, and K. Skrzypkowski, "Investigation of selected surface topography parameters and deformation during milling of vertical thin-walled structures from titanium alloy Ti6Al4V," Materials, vol. 16, art. 3182, 2023, https://doi.org/10.3390/ma16083182

[25] A. A. Lassila, D. Svensson, W. Wang, et al., “Numerical evaluation of cutting strategies for thin-walled parts,” Scientific Reports, vol. 14, art. 1459, 2024, https://doi.org/10.1038/s41598-024-51883-1

[26] M. Lin et al., “Deformation prediction in flank milling of thin-walled parts based on cutter-workpiece engagement,” Journal of Manufacturing Processes, vol. 115, pp. 375-386, 2024, https://doi.org/10.1016/j.jmapro.2024.02.013

[27] N. T. Anh and T. T. Tung, “Finite element and experimental investigation of up- and down-milling in thin-wall machining,” Progress in Engineering Science, vol. 3, art. 100209, 2026, https://doi.org/10.1016/j.pes.2026.100209

[28] I. Llanos et al., “Deflection error modeling during thin-wall machining,” Procedia CIRP, vol. 117, pp. 169-174, 2023, https://doi.org/10.1016/j.procir.2023.03.030

[29] D.-M. Shi et al., “An explicit coupling model for accurate prediction of force-induced deflection in thin-walled workpiece milling,” Journal of Manufacturing Science and Engineering, vol. 144, no. 8, art. 081005, 2022, https://doi.org/10.1115/1.4053682

[30] Q. Sun, J. Zhou, and P. Li, “Simulations and experiments on the micro-milling process of a thin-walled structure of Al6061-T6,” Materials, vol. 15, art. 3568, 2022, https://doi.org/10.3390/ma15103568

[31] S. Umashankar, H. V. Manjunath, and C. S. Sumesh, “Experimental and numerical optimization of process parameters for thin wall machining of bearing housings,” Materials Today: Proceedings, vol. 46, pp. 4925-4934, 2021, https://doi.org/10.1016/j.matpr.2020.10.336

[32] D. Weber et al., “Investigation on the scale effects of initial bulk and machining-induced residual stresses of thin-walled milled monolithic aluminum workpieces on part distortions,” Procedia CIRP, vol. 102, pp. 337-342, 2021, https://doi.org/10.1016/j.procir.2021.09.058

[33] D. Weber et al., “Simulation-based compensation techniques to minimize distortion of thin-walled monolithic aluminum parts due to residual stresses,” CIRP Journal of Manufacturing Science and Technology, vol. 38, pp. 427-441, 2022, https://doi.org/10.1016/j.cirpj.2022.05.016

[34] G. Yao and Z. Liu, “Analytical modelling for residual stress prediction in multi-step side milling of GH4169 thin-wall parts based on deformation,” Journal of Materials Research and Technology, vol. 32, pp. 1984-1995, 2024, https://doi.org/10.1016/j.jmrt.2024.08.042

[35] B. Li, S. N. Melkote, and S. Y. Liang, “Analysis of reactions and minimum clamping force for machining fixtures with large contact areas,” International Journal of Advanced Manufacturing Technology, vol. 16, pp. 79-84, 2000.

[36] T. T. Tung, N. T. Anh, N. X. Quynh, and T. V. Minh, “Development of a machining allowance model for rectangular pocket milling operations,” Revista de Ciencias Tecnológicas, vol. 9, no. 3, art. e498, 2026, https://doi.org/10.37636/recit.v9n3e498

[37] M. Soori, F. K. Jough, R. Dastres, and B. Arezoo, “Robotic automation in CNC machine tools: A review,” Acta Mechanica et Automatica, vol. 18, no. 3, pp. 434-450, 2024.

[38] T. T. Tung, N. X. Quynh, and T. V. Minh, “Experimental optimization of cutting parameters in flat-surface end milling using the Taguchi-desirability approach,” Engineering, Technology & Applied Science Research, vol. 16, no. 3, pp. 36693-36699, 2026, https://doi.org/10.48084/etasr.18640

[39] K. H. Ho and S. T. Newman, “State of the art electrical discharge machining (EDM),” International Journal of Machine Tools and Manufacture, vol. 43, no. 13, pp. 1287-1300, 2003, https://doi.org/10.1016/S0890-6955(03)00162-7